RAA 2016 Vol. **16** No. **2**, 34 (8pp) doi: 10.1088/1674–4527/16/2/034
http://www.raa-journal.org *http://iopscience.iop.org/raa*

***R**esearch in*
***A**stronomy and*
***A**strophysics*

An active M star with X-ray double flares disguised as an ultra-luminous X-ray source

Jin-Cheng Guo[1,2], Ji-Feng Liu[1], Song Wang[1], Yue Wu[1] and Yu-Xiang Qin[3]

[1] Key Laboratory of Optical Astronomy, National Astronomical Observatories, Chinese Academy of Sciences, Beijing 100012, China; *jcguo@nao.cas.cn*
[2] University of Chinese Academy of Sciences, Beijing 100049, China
[3] School of Physics, The University of Melbourne, Parkville, Victoria 3010, Australia

Received 2015 July 31; accepted September 7

Abstract Here we present research on an ultra-luminous X-ray source (ULX) candidate 2XMM J140229.91+542118.8. The X-ray light curves of this ULX candidate in M101 exhibit features of a flare star. More importantly, the *Chandra* light curve displays unusual X-ray double flares, which is comprised of two close peaks. The X-ray (0.3–11.0 keV) flux of the first peak was derived from the two-temperature APEC model as $\sim 1.1 \pm 0.1 \times 10^{-12}\ \mathrm{erg\,cm^{-2}\,s^{-1}}$. The observed flux at its first peak increased by about two orders of magnitude in X-ray as compared to quiescence. The slope of the second fast decay phase is steeper than the slope of the first fast decay phase, indicating that the appearance of a second flare accelerated the cooling of the first flare in a way we do not understand yet. We also observed its optical counterpart using a 2.16 m telescope administered by National Astronomical Observatories, Chinese Academy of Sciences. By optical spectral fitting, it is confirmed to be a late type dMe2.5 star. According to the spectral type and apparent magnitude of its optical counterpart, we estimate the photometric distance to be $\sim 133.4 \pm 14.2$ pc. According to the X-ray spectral fitting, a possible explanation is provided. However, more similar close double flares are needed to confirm whether this accelerated cooling event is a unique coincidence or a common physical process during double flaring.

Key words: stars: flare — X-ray: stars — galaxies: individual (M101)

1 INTRODUCTION

Non-nuclear ultra-luminous X-ray sources (ULXs) in nearby galaxies are X-ray sources with observed luminosities greater than $10^{39}\ \mathrm{erg\ s^{-1}}$, which is comparable to the Eddington luminosity of a $\sim 10\ M_{\odot}$ black hole. Recent research has indicated ULXs are accreting black holes that may contain the missing population of intermediate mass black holes or reflect super-Eddington accretion physics (Feng & Soria 2011). Three classes of black holes are thought to be able to power ULXs: normal stellar mass black holes ($\sim 10\ M_{\odot}$), massive stellar mass black holes ($\leq 100\,M_{\odot}$), and intermediate mass black holes (10^2 – $10^4\ M_{\odot}$). Since the merger of intermediate mass black holes may be the most likely channel to form a supermassive black hole, the study of this missing link and its best candidate, the ULX, is crucial.

In recent studies, most of the ULX catalogs were made by searching for non-nuclear X-ray point sources in nearby galaxies (Liu 2011; Walton et al. 2011). Therefore, contaminations like active foreground stars, background quasars, AGNs and even some X-ray bright supernovae were introduced (Heida et al. 2013). If the ULX has an optical counterpart, then the optical spectrum can help us to confirm whether it is a ULX or contaminant source.

M101 is a nearby grand design spiral galaxy with a number of ULXs. Among these, 2XMM J140229.91+542118.8 (RA = 14:02:30, Dec = +54:21:18; hereafter 2X J1402+54) is one ULX candidate identified by several ULX catalogs. Wang et al. (1999) included 2X J1402+54 as an X-ray source in M101 based on a *ROSAT* image. The authors associated 2X J1402+54 with a star that is offset by 4.1″ and footnoted this source as detection confused with a nearby object. Then it was first identified as a ULX source in Swartz et al. (2004) with the observed and intrinsic luminosities of $0.81 \pm 0.12 \times 10^{39}\ \mathrm{erg\ \ s^{-1}}$ and $1.43 \pm 0.05 \times 10^{39}\ \mathrm{erg\ \ s^{-1}}$, respectively. Colbert et al. (2004) included this source as an X-ray point source as well, whose X-ray luminosity of 0.3–8 keV was determined as $0.794 \times 10^{39}\,\mathrm{erg\,s^{-1}}$. Later, Feng & Kaaret (2005) claimed this source is a young supernova remnant based on X-ray spectral fitting. More recently, Lin et al. (2012) classified this source as a star using an *XMM-Newton* observation. However, Mineo et al. (2012) identi-

fied 2X J1402+54 as a high-mass X-ray binary based on *Chandra* data.

In addition, this source also has an optical counterpart (Pineau et al. 2011), which was identified by cross-correlation of the 2XMMi catalog with Data Release 7 of the Sloan Digital Sky Survey (SDSS DR7). According to the photometry of SDSS DR7, the apparent magnitudes are $u = 18.886 \pm 0.020$ mag, $g = 16.578 \pm 0.004$ mag, $r = 15.083 \pm 0.004$ mag, $i = 15.706 \pm 0.013$ mag and $z = 13.010 \pm 0.004$ mag. Nevertheless, optical spectroscopic observations that verify its nature are lacking.

Our recent inspection of this source's light curve revealed flares reminiscent of late-type active stars. Therefore, we carried out detailed studies to verify its nature. In Section 2 we describe light curves and X-ray spectral analysis observed by *Chandra*. The optical spectrum and classification will be presented in Section 3. In Section 4 discussions and conclusions are presented.

2 THE OBSERVATIONS AND X-RAY LIGHT CURVES

The source 2X J1402+54 is located $6'$ west of the nucleus of M101. As a famous face-on spiral galaxy 6–7 Mpc away from us (Shappee & Stanek 2011; Lee & Jang 2012), M101 has been observed by *XMM-Newton* three times and more than 20 times by *Chandra*.

Among these observations, observations ACIS934 and ACIS4732 captured obvious X-ray flare events. Observation ACIS934 was made on 2000 March 26 with a 98.38 ks exposure. Observation ACIS4732 was carried out on 2004 March 19 with a 69.79 ks exposure. However, due to the relatively low count rate of observation ACIS934, only observation ACIS4732 was analyzed specifically in this paper. All *Chandra* data used in this paper were obtained and processed with *Chandra* Interactive Analysis of Observations (CIAO) software (Fruscione et al. 2006) version 4.5.

The entire X-ray flare event on 2004 March 19 was captured by *Chandra* ACIS-S in observation 4732. The 0.1–8.0 keV X-ray light curve with 1000 s binning is presented in Figure 1. Time $t = 0$ corresponds to 2004 March 19 UT 08:14 when it is still in the quiescent state with count rate level around 0.01 $\mathrm{counts\ s^{-1}}$. In order to analyze the X-ray light curve in detail, exponential fits are applied to the decay phases. Based on the different slopes of these exponential fits on a logarithmic scale, this flare can be divided into several phases which are labeled in Figures 1 and 2. The quiescent state (Q) of the source persisted during the first two hours. Then a rapid rise occurred, during which the count rate increased by about 17 times. This is referred to as the first rise phase (R1). After that are a fast decay phase (D1) and a short slow decay phase (D2). However, there appeared to be a second flare whose slope of the fast decay phase is even steeper than that of the first fast decay. The time boundaries of quiescent (Q), first rise (R1), first fast decay (D1), first slow decay (D2), second rise (R2) and second fast decay (D3) are marked by red vertical lines in Figure 1.

The X-ray spectrum of 2X J1402+54 was examined by Feng & Kaaret (2005). They fitted this source with a power law model and a multicolor disk (MCD) component using XSPEC. However, the residuals of fitting are significant, and χ^2/dof (degree of freedom) of the fitting is 160.7/86 = 1.8686. On the other hand, the spectrum shows a bump around 0.5–1.0 keV, a region where hot diffuse gas usually produces significant line emission. Therefore, they tried a power law plus Mekal model (Mewe et al. 1995) which is a hot diffuse thermal plasma model. This combination yields a much better fit with spectral parameter $kT = 0.67 \pm 0.04$ keV and χ^2/dof = 115.5/86 = 1.343. The presence of the Mekal component suggests that part of the X-ray emission arises from hot diffuse thermal plasma. The fraction of the total luminosity in the Mekal component is 31.7% according to their research. Feng & Kaaret (2005) provided one plausible interpretation for the hot diffuse plasma component that regards this source as a young supernova remnant.

In order to study the specific physical properties of this flare event, we have investigated the X-ray spectra of the flare in each phase except for spectra from the R2 phase, owing to its very low number of photons, 94. We first used CIAO to extract different phases from the original event file. Then spectra were extracted for X-ray spectral fitting. Once the spectra of different phases were obtained, the single-temperature (1T) and two-temperature (2T) thermal emission APEC models (Smith et al. 2001) were applied to fit the spectra. The solar abundance was used, since our attempt to vary the abundance leads to unrealistic parameter values and no significant improvement in the fitting result. The 2T model was found to produce much better fits than the 1T model for all the phases, even including the quiescent phase. The best fit parameters of all phases are summarized in Table 1 which was fitted by the X-ray package XSPEC (Dorman & Arnaud 2001). One can also find the best fit spectrum and associated residuals in Figure 3.

Due to the relatively low count rate ($\sim 0.17\,\mathrm{count\ s^{-1}}$ at the flare peak) of this observation, the line-of-sight neutral hydrogen column density $(N_{\rm H})$ could not be well constrained by the fitting. On the other hand, according to calculation with the program NH from HEASOFT ($N_{\rm H}$ value derived from the HI map by Kalberla et al. 2005), the average $N_{\rm H}$ from the direction (14:02:30, +54:21:18) is $1.39 \times 10^{20}\ \mathrm{cm^{-2}}$. This result suggests that the actual $N_{\rm H}$ value of this source is much less than $1.39 \times 10^{20}\ \mathrm{cm^{-2}}$, which is already too low to introduce significant changes to the fitted plasma temperature. Therefore, the average $N_{\rm H}$ value is adopted during the fitting.

In Table 1, we fitted each phase with the 2T APEC model while $N_{\rm H}$ was fixed at $1.39 \times 10^{20}\mathrm{cm^{-2}}$, even including the quiescent phase which is due to "microflar-

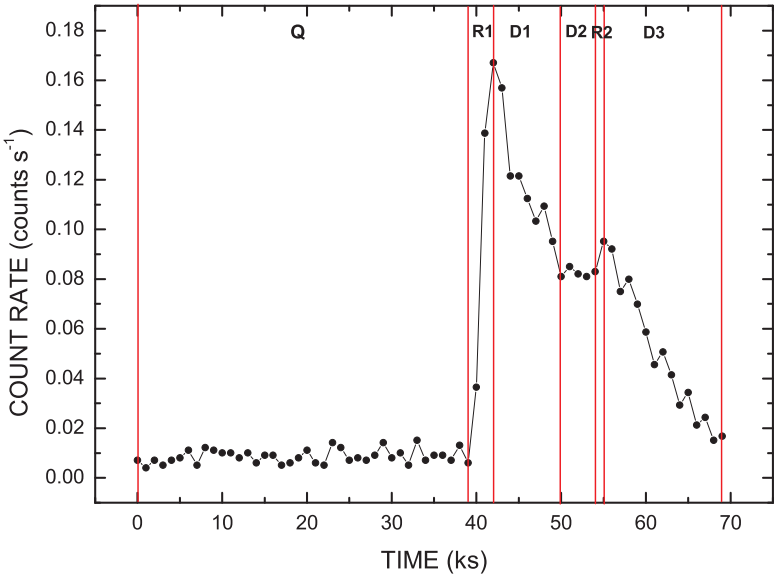

Fig. 1 The light curve for observation 4732 detected by the *Chandra* ACIS detector on 2004 March 19–20. A time bin of 1000 s is adopted here for a better light curve fit and visualization. The whole observation has been divided into phases of quiescent, first rise, first fast decay, first slow decay, second rise and second fast decay, which are labeled as Q, R1, D1, D2, R2 and D3, respectively.

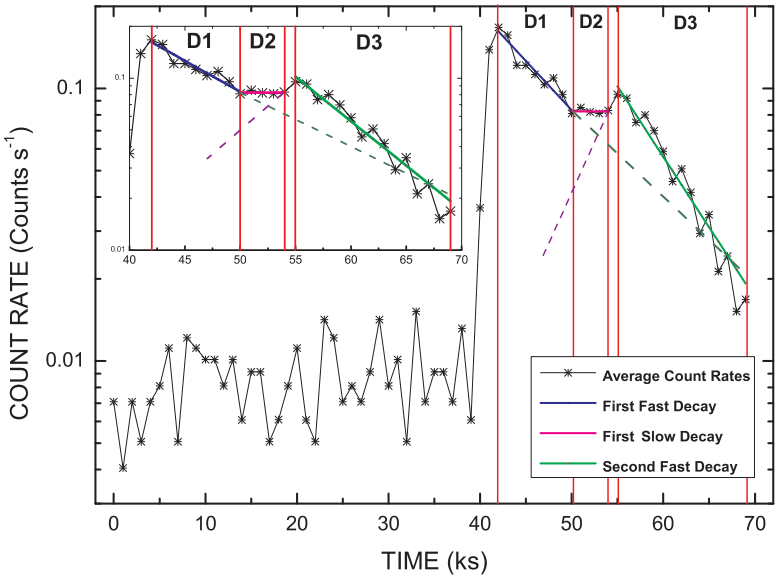

Fig. 2 The light curve of detection ACIS4732 was fitted with an exponential for the decay phases, plotted on a logarithmic scale. The blue line, pink line and green line are the exponential fits for D1, D2 and D3, respectively. As this figure shows, the slope of D2 is rather flat and the slope of D3 is steeper than the slope of D1. The green and purple dashed lines are an extension of exponential fits for the D1 and R2 phases respectively. These two lines are intended to give one a rough idea about what the decay of a first flare and the rise of a second flare would be like.

ing" (for more details see Sect. 4). However, the values of reduced χ^2 for the Q and D3 phases are not very good. Scrutinizing the X-ray spectrum, we believe it is caused by the presence of several emission lines.

3 OPTICAL SPECTRAL ANALYSIS

After analyzing the X-ray spectra and light curve of the source 2X J1402+54, a 2.16 m telescope administered by National Astronomical Observatories, Chinese Academy of Sciences (NAOC) at Xinglong Observing Station was used to obtain its optical spectrum in order to further confirm our speculation. The optical spectra were taken on 2013 July 02 and 03 with the BAO Faint Object Spectrograph and Camera in the 2.16 m aperture of the reflecting telescope. G4 and G8 grisms were both used in this observation along with a long slit approximately $2''$ in width. This source was observed for two nights, and we

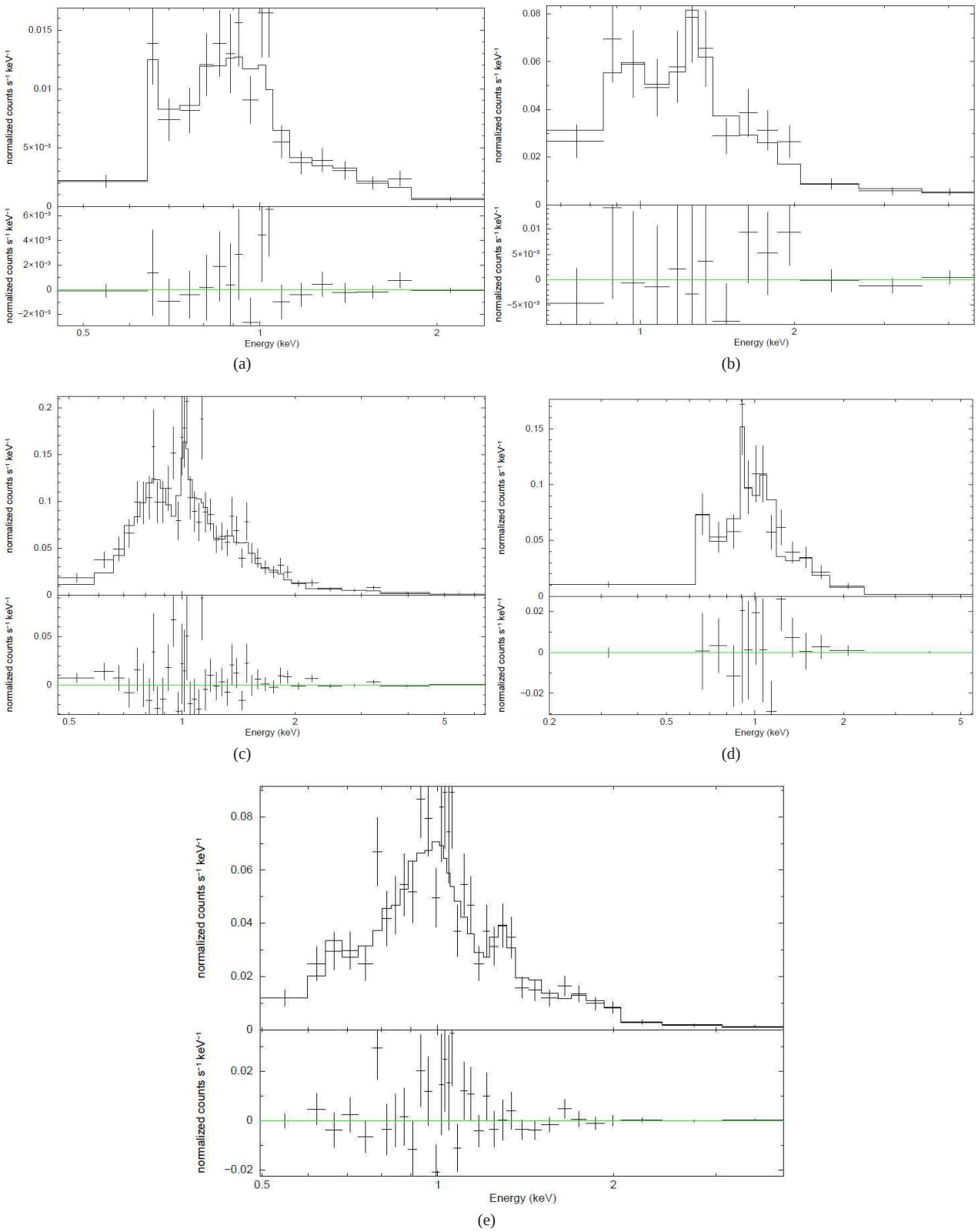

Fig. 3 The results of spectral fitting for each phase using the 2T APEC model and Gaussian fit. The phase of Q, R1, D1, D2 and D3 correspond to top left, top right, middle left, middle right and bottom, respectively. As the spectra show, there are several emission lines around 1 keV that produce large residuals.

Table 1 Spectral fitting results of 2X J1402+54's flare with the *Chandra* detection ACIS4732 (The flux (0.3–11.0 keV) is in units of 10^{-13} erg cm^{-2}s^{-1}, and the luminosity is in units of 10^{30} erg s^{-1}).

Phase	Duration (ks)	$N_{\rm H}$ (10^{20} cm^{-2})	$kT1$ (keV)	$kT2$ (keV)	$kT3$ (keV)	χ^2_υ (dof)	Flux	Luminosity	Counts
Q	40	1.39	0.299 ± 0.029	1.228 ± 0.076	—	1.862(14)	0.61	0.13	345
Q[a]	40	0.0139	0.312 ± 0.028	1.232 ± 0.076	—	1.870(14)	0.61	0.13	345
R1	3	1.39	0.955 ± 0.225	8.600 ± 4.838	—	1.240(10)	10.67	2.27	344
D1	8	1.39	0.763 ± 0.049	3.003 ± 0.317	—	1.518(38)	9.23	1.97	1055
D2	4	1.39	0.220 ± 0.025	1.616 ± 0.098	—	1.272(12)	7.17	0.58	489
R2	1	—	—	—	—	—	—	—	94
D3	14	1.39	0.951 ± 0.046	3.063 ± 0.665	—	2.081(31)	3.67	0.78	740
D3[b]	14	1.39	0.239 ± 0.034	1.043 ± 0.054	3.439 ± 1.089	1.549(29)	1.178	0.25	740

Notes: [a] After distance was estimated, we tried a much lower $N_{\rm H}$ to check the influence of fixed $N_{\rm H}$. [b] Due to the unsatisfying χ^2 of 2T APEC for the D3 phase, we also tried a three-temperature model with APEC. The result yields a better fit and consistent parameters.

acquired two 1800 s exposures each night. The wavelength calibrations were carried out using Fe/Ar lamps. The software package IRAF (Tody 1986) was applied to perform the standard CCD procedures including overscan and bias subtraction, flat correction, cosmic-ray removal, spectral extraction and wavelength calibration. The sky emission lines were masked for stellar atmosphere parameter fitting.

The stellar atmosphere model based on ELODIE (Prugniel & Soubiran 2001; Prugniel et al. 2007; Wu et al. 2011) and the fitting tool ULySS (Koleva 2009; Wu et al. 2014; Wu et al. 2011) were adopted to fit the spectra.

First, the two spectra were fitted separately; then, the two observations were combined and fitted by the model. The observation taken on July 02 was best fitted with the parameters of

$$T_{\rm eff} = 3469\,{\rm K}, \quad \log g = 5.0 \quad \text{and} \quad [{\rm Fe/H}] = -1.3;$$

the observation taken on July 03 was best fitted with parameters of

$$T_{\rm eff} = 3509\,{\rm K}, \quad \log g = 5.0 \ \text{and} \ [{\rm Fe/H}] = -1.2\,.$$

The combined spectrum was best fitted with the parameters of

$$T_{\rm eff} = 3479\,K, \quad \log g = 5.0 \quad \text{and} \quad [{\rm Fe/H}] = -1.1\,.$$

The optical spectral fitting indicates that the source 2X J1402+54 is a dMe2.5 dwarf star (Fig. 4).

Based on the spectral type M2.5V, we derived the approximate photometric distance. First, we linearly interpolated the spectral type M2.5V to obtain the absolute magnitudes for SDSS $ugriz$ bands from table 3 of Covey et al. (2007). Then, the averaged distance is calculated to be about 133.4 ± 14.2 pc. This distance is applied to obtain the luminosity in Table 1. Due to the very close distance of the star, we re-fixed the $N_{\rm H}$ to 1.39×10^{18} cm^{-2} to check if there is any significant change in the X-ray spectral fit. The result in Table 1 for the Q phase demonstrates it has a similar outcome.

4 DISCUSSION AND CONCLUSION

During the X-ray light curve and X-ray spectral analysis, two facts are worth noticing. One is that the X-ray spectral fitting of the quiescent phase required the 2T thermal plasma emission model instead of the usual 1T model. Normally during the quiescent phase, it is generally believed that there are no flare events. In this case, the emission will only be generated from the stellar chromospheres' background radiation which stays at almost the same temperature. Hence, a 1T plasma emission model is sufficient to fit the quiescent phase spectrum. However, this is not our case. Although the 1T fit gives a reduced $\chi^2 = 2.688$, the 2T model provides a better fit with a reduced $\chi^2 = 1.862$. This can be explained well by the concept of quiescent "microflaring." Several studies (Butler et al. 1986; Ambruster et al. 1987; Robinson et al. 1995; Audard et al. 2000; Kashyap et al. 2002; Güdel et al. 2003; Wargelin et al. 2008) have suggested that the apparently quiescent emission from the stellar corona may be due to the continuous eruption of small flares, commonly referred to as "microflaring." The luminosity of these microflares is roughly 10^{26}–10^{29} erg s^{-1}.

Another notable fact is the special cooling process indicated by the X-ray light curve which is illustrated in Figure 2. During observation ACIS4732, there was a rapid rise in the first giant flare, followed by a normal fast decay phase and an extremely flat slow decay phase. After that was a second flare with an even steeper slope than the fast decay of the first one. We can even find that during the last few kiloseconds of this observation, the fast decay of the second flare became steeper than our exponential fit, as shown in Figure 3.

Actually, double X-ray flare events have been reported several times. For example, Katsova et al. (1999) reported the first detection of post eruptive energy release on a red dwarf star. They concluded that this double flare event closely resembles a system of giant coronal arches that

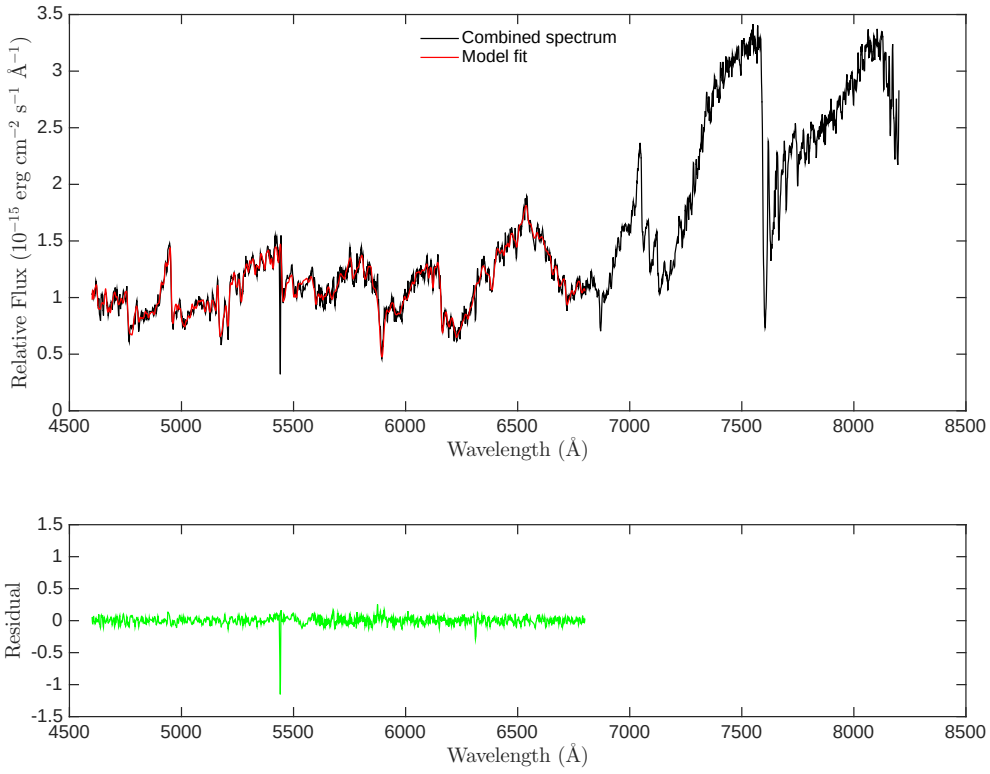

Fig. 4 Optical spectrum obtained from the 2.16 m telescope administered by NAOC. Top panel: The black line is the combined spectrum while the red line is the best ELODIE model fit. (The ELODIE model only covers the range to 6800 Å at the red end.) Bottom panel: Residuals from the spectral fitting; the unit is 10^{-15} erg cm^{-2} s^{-1} Å^{-1}. Best fit parameters: $T_{\rm eff} = 3479$ K, $\log g = 5.0$ and $[{\rm Fe/H}] = -1.1$. The optical spectral fitting indicates that this source is a dMe2.5 star.

form after a coronal mass ejection occurs on our Sun. Such a system would be energized by reconnection in a vertical current sheet. Favata et al. (2000) analyzed an extreme X-ray flare observed by *ASCA*. This 150 ks observation included at least three individual flares, two of which were minor flares right after the major one.

Reale et al. (2004) modeled an X-ray flare on Proxima Centauri observed by *XMM-Newton*, and they claimed that this flare can be well described with two components: the first major one triggered by an intense heat pulse injected in a single flaring loop, followed by a less intense heat pulse half an hour later which was also released in the related loop system.

Trenholme et al. (2004) presented the results of a search for stellar X-ray flares using the XMM-Newton public data archive of stellar X-ray flares, and found that one source shows two flares in close succession, which was then compared to solar flares. The solar flares can be described in a sympathetic or homologous way. Sympathetic flares are believed to appear when a flare initiates a shock front, which propagates to another active region, causing that active region to flare. These disturbances are known as Moreton waves (Moreton 1964). Homologous flares are caused by the recurrent destruction and reformation of stellar magnetic fields, driven by the constant action of emerging flux and/or magnetic shear (Martres et al. 1984). This kind of process usually produces flares with similar magnitude and emission measure which originate from the same active region. After calculation and deduction, they concluded the formation of this double flare is more likely to be homologous and from the same active region.

According to a comparison of the morphology of these four double flares, we were able to find some similarities. For instance, the extremely flat slow decay phase of the flare we found in the *Chandra* observation resembles the R2 phase of the double flare from Reale et al. (2004). We think they are both flat and maintain at a relatively high count rate level because another loop begins to flare. The rising emission of the second flare overlapped the emission of the first loop, and slowed down the decay of the first one. That also affected the rise profile of the second flare, and that is the reason why the slow decay phase is so flat and the R2 phase is so minor and has a very short duration. Nevertheless, the behavior of the fast decay of our second flare is still hard to understand. Due to relatively low count rates (less than 0.18 at the higher

peak), we were not able to investigate further properties (e.g. physical size) of the flare.

Even though the mechanism causing the acceleration of the cooling process in the second decay remains unknown to us, we have speculated about this whole process. After the first flare generated a shock front which is a disturbance in the corona, it propagated to another active region nearby. The shock caused that active region to flare as well, which occurred when the first flare was going through the slow decay phase. Hence, the rapid rising phase of the second flare overlapped with the slowly decaying phase of the first flare. That leads to the extremely flat D2 phase in the light curve. According to our X-ray spectral fitting, we have one possible explanation for the accelerated cooling of the D3 phase, which is closely related to the presence of the third temperature component. That third component is most likely to be the residual emission of the first flare. Due to certain reasons like rotation of the star or the rapid energy transmission from the first flare to the second, this third temperature component suddenly disappeared during the last few kiloseconds of the observation. However, the explanation of rotation requires much fine-tuning. Therefore, more similar close double flare events are needed to investigate whether this is a unique coincidence or a common physical process during double flaring.

In this work, a ULX candidate identified by several ULX catalogs is studied in detail. Its *Chandra* light curves show obvious flares and one of them is comprised of two close double flares. The X-ray spectra of each phase from the double peak flare were fitted with the 2T APEC model fairly well, suggesting the X-ray emission from this source arises from hot diffuse thermal plasma. By optical spectra fitted with an ELODIE model, 2X J1402+54 is determined to be a dMe2.5 star. With an estimated distance of 133.4 ± 14.2 pc, the luminosity of the this source is actually around 10^{30} erg s^{-1}. Therefore, it is indeed a foreground flare star instead of a ULX or high mass X-ray binary. Also with the help of an X-ray spectral fitting, we provide a possible explanation for the close double flares and peculiar accelerated cooling process captured by *Chandra*'s light curve. However, the rotation scenario requires much fine-tuning. We are planning to systematically search for close double flare events in *Chandra* and *XMM-Newton* data in order to further investigate the mechanism behind this kind of special cooling process.

Acknowledgements The authors would like to thank the anonymous referee for the helpful suggestions. The authors acknowledge the National Natural Science Foundation of China (NSFC) under grants 11333004 and 11403056. This research has made use of the SIMBAD database, operated at CDS, Strasbourg, France.

References

Ambruster, C. W., Sciortino, S., & Golub, L. 1987, ApJS, 65, 273
Audard, M., Güdel, M., Drake, J. J., & Kashyap, V. L. 2000, ApJ, 541, 396
Butler, C. J., Rodono, M., Foing, B. H., & Haisch, B. M. 1986, Nature, 321, 679
Colbert, E. J. M., Heckman, T. M., Ptak, A. F., Strickland, D. K., & Weaver, K. A. 2004, ApJ, 602, 231
Covey, K. R., Ivezić, Ž., Schlegel, D., et al. 2007, AJ, 134, 2398
Dorman, B., & Arnaud, K. A. 2001, in Astronomical Society of the Pacific Conference Series, 238, Astronomical Data Analysis Software and Systems X, eds. F. R. Harnden, Jr., F. A. Primini, & H. E. Payne, 415
Favata, F., Reale, F., Micela, G., et al. 2000, A&A, 353, 987
Feng, H., & Kaaret, P. 2005, ApJ, 633, 1052
Feng, H., & Soria, R. 2011, New Astron. Rev., 55, 166
Fruscione, A., McDowell, J. C., Allen, G. E., et al. 2006, in Society of Photo-Optical Instrumentation Engineers (SPIE) Conference Series, 6270, 1
Güdel, M., Arzner, K., Audard, M., & Mewe, R. 2003, A&A, 403, 155
Heida, M., Jonker, P. G., Torres, M. A. P., et al. 2013, MNRAS, 433, 681
Kalberla, P. M. W., Burton, W. B., Hartmann, D., et al. 2005, A&A, 440, 775
Kashyap, V. L., Drake, J. J., Güdel, M., & Audard, M. 2002, ApJ, 580, 1118
Katsova, M. M., Drake, J. J., & Livshits, M. A. 1999, ApJ, 510, 986
Koleva, M., Prugniel, P., Bouchard, A., & Wu, Y. 2009, A&A, 501, 1269
Lee, M. G., & Jang, I. S. 2012, ApJ, 760, L14
Lin, D., Webb, N. A., & Barret, D. 2012, ApJ, 756, 27
Liu, J. 2011, ApJS, 192, 10
Martres, M.-J., Mein, N., Mouradian, Z., et al. 1984, Advances in Space Research, 4, 5
Mewe, R., Kaastra, J. S., Schrijver, C. J., van den Oord, G. H. J., & Alkemade, F. J. M. 1995, A&A, 296, 477
Mineo, S., Gilfanov, M., & Sunyaev, R. 2012, MNRAS, 419, 2095
Moreton, G. F. 1964, AJ, 69, 145
Pineau, F.-X., Motch, C., Carrera, F., et al. 2011, A&A, 527, A126
Prugniel, P., & Soubiran, C. 2001, A&A, 369, 1048
Prugniel, P., Soubiran, C., Koleva, M., & Le Borgne, D. 2007, astro-ph/0703658
Reale, F., Güdel, M., Peres, G., & Audard, M. 2004, A&A, 416, 733
Robinson, R. D., Carpenter, K. G., Percival, J. W., & Bookbinder, J. A. 1995, ApJ, 451, 795
Shappee, B. J., & Stanek, K. Z. 2011, ApJ, 733, 124
Smith, R. K., Brickhouse, N. S., Liedahl, D. A., & Raymond,

J. C. 2001, ApJ, 556, L91
Swartz, D. A., Ghosh, K. K., Tennant, A. F., & Wu, K. 2004, ApJS, 154, 519
Tody, D. 1986, in Society of Photo-Optical Instrumentation Engineers (SPIE) Conference Series, 627, Instrumentation in Astronomy VI, ed. D. L. Crawford, 733
Trenholme, D., Ramsay, G., & Foley, C. 2004, MNRAS, 355, 1125
Walton, D. J., Roberts, T. P., Mateos, S., & Heard, V. 2011, MNRAS, 416, 1844
Wargelin, B. J., Kashyap, V. L., Drake, J. J., García-Alvarez, D., & Ratzlaff, P. W. 2008, ApJ, 676, 610
Wu, Y., Singh, H. P., Prugniel, P., Gupta, R., & Koleva, M. 2011, A&A, 525, A71
Wu Y., et al. 2014; (2014IAUS..306..340W)
http://adsabs.harvard.edu/abs/2014IAUS..306..340W
Wu, Y., Luo, A. L., Li, H. N., et al. 2011, RAA (Research in Astronomy and Astrophysics), 11, 924